BOREAL ENVIRONMENT RESEARCH 17: 193–209
ISSN 1239-6095 (print) ISSN 1797-2469 (online)

Helsinki 29 June 2012

Forest-edge effects on sea-salt aerosol deposition: a wind-tunnel study using living oak leaves

Ausra Reinap[1)2)], Bo L.B. Wiman[1)], Birgitta Svenningsson[2)] and Sara Gunnarsson[1)]

[1)] *Environmental Science & Technology Section, School of Natural Sciences, Linnaeus University, Barlastgatan 11, SE-391 82 Kalmar, Sweden*
[2)] *Department of Physics, Lund University, P.O. Box 118, SE-221 00 Lund, Sweden*

Received 25 Feb. 2011, final version received 24 Oct. 2011, accepted 15 Sep. 2011

Reinap, A., Wiman, B. L. B., Svenningsson, B. & Gunnarsson, S. 2012: Forest-edge effects on sea-salt aerosol deposition: a wind-tunnel study using living oak leaves. *Boreal Env. Res.* 17: 193–209.

Landscape patchiness creates aerodynamic transition zones that affect the exchange of nutrients and pollutants between the atmosphere and vegetation. Using an artificially-generated NaCl aerosol (mass-*versus*-particle-size distribution with aerodynamic mean particle diameter 1.6 μm; geometric standard deviation 1.9), we investigated the forest-edge effect on aerosol deposition within a model oak (*Quercus robur*) canopy in a wind tunnel with an emulated beach-to-forest transition. The deposition rate around the forest edge was 2–3 times higher than to the beach and 50%–60% higher than to the interior of the forest. The deposition velocity at the edge was 0.06 cm s^{-1}, which is 2–3 times higher than the beach-deposition velocity. Our results can help improve estimates of aerosol-borne inputs of nutrients or pollutants to forested landscapes that experience shifts in meteorological regimes due to changes in climate and forestry practices, in particular with respect to deciduous species in coastal environments.

Introduction

Forest edges create aerodynamic transition zones that affect the exchange of mass and momentum between the atmosphere and vegetation (Wiman and Ågren 1985, Wiman and Lannefors 1985, Lindberg and Owens 1993, Draaijers *et al*. 1994, Ould-Dada 2002, Erisman *et al*. 2003, Wuyts *et al*. 2008a, 2008b). In particular, in a changing climate, coastal forests are likely to receive increasing amounts of deposits of marine aerosols and pollutants (cf. e.g., Gustafsson and Franzén 2000, Wiman *et al*. 2003) affecting nutrient turnover as well as posing risks.

Modelling and quantification of aerosol deposition to forest walls are becoming increasingly important tasks in view of climatic changes (Solomon *et al*. 2007) and shifts in land-use (Bodin and Wiman 2007). Methods to investigate edge effects on deposition processes *in situ* face limitations and difficulties, however. For instance, deposition patterns arising in complex terrain cannot be quantified by conventional micrometeorological methods (Hicks *et al*. 1989). Aerosol-deposition models require several types of input data on factors in operation along transects from aerodynamically relatively smooth (such as coastal waters) to rough (coastal forests) surface structure character-

Editor in charge of this article: Veli-Matti Kerminen

istics. Wind-tunnel studies can help address these problems through providing controlled conditions with a focus on leaf-surface morphology and aerosol composition (Reinap *et al*. 2009, Fowler *et al*. 2009). In particular, wind-tunnel experiments by Wuyts *et al*. (2008a) support the existence of edge effects which affect deposition processes and provide information on the influence of edge structure. Previous studies (Lindberg and Owens 1993, Ould-Dada 2002, Wuyts *et al*. 2008b) also revealed enhanced deposition at forest edges and pointed out the importance of meteorological factors as well as canopy-edge structural elements for deposition mechanisms around forest fringes.

The major objective of the present study was to assess whether the effect of edge on aerosol deposition within an oak canopy ("forest model") downwind of a smooth surface ("beach model") in a wind tunnel was observable and quantifiable. Oak was chosen because it is a common species in coastal environments in Europe (cf. e.g. Skjøth *et al*. 2008) and because deposition to edges in deciduous forests has been little explored in comparison with that in coniferous ones. In addition, most empirical studies of deposition around forest edges are based on throughfall techniques and do not clearly separate the contribution by aerosols from that by other processes that might be enhanced at edges (such as increased leaching from forest walls exposed to high wind speeds and solar irradiation, and increased gaseous deposition). In our experiments, the focus was on the aerosol part of the edge effect. Our research questions also included whether aerosol-capture efficiencies differed between cultivated and field oaks. We used NaCl aerosol generated using a modified bubble-bursting technique, and also aimed to explore whether particle-size distributions could be generated that would help establish relationships between deposition and particle size. Our results provide quantitative estimates of deposition rates within the emulated beach-to-forest transition. Deposition rates per unit ground surface area and per unit time and unit leaf surface area are addressed.

Theory

Aerosol dry deposition is determined by several factors, including particle size, wind speed, mechanical and thermal turbulence, canopy structure (including Leaf Area Index, LAI), leaf geometry and morphology (such as needle and leaf dimensions, leaf hairiness) and leaf-surface wetness (*see* e.g. Wiman and Ågren 1985, Reinap *et al*. 2009). Also, leaf-surface stickiness plays a role. At low stickiness of the collecting surface and at high wind speeds occurring more frequently at forest edges than in forest interiors, particle re-suspension might be intense (Wu *et al*. 1992, Ould-Dada 2002). The effect of edge on particle deposition implies a phenomenon of transition from a relatively smooth surface to more complex and aerodynamically rough structures, and wind entering the forest at its edge induces a pressure gradient, the magnitude of which reflects turbulence and wind velocity (Wiman and Ågren 1985). Enhanced deposition at a forest edge can, therefore, be related to a change in the surface roughness length (z_o), zero plane displacement (d) and friction velocity (u), and an increased turbulence. The roughness length is often found to increase linearly with stand height and canopy closure (Draaijers 1993).

The drag force on air volumes moving through the forest is highly dependent on leaf area density (leaf surface area per unit air volume in the forest) which can be integrated over the forest height to give leaf surface area per unit ground-surface area (i.e. LAI). In the turbulent boundary layer around the edge, and above the canopy, transfer of momentum and mass is determined by diffusivities associated with turbulent eddies (Monteith and Unsworth 1990). Such "eddy diffusivities" are many orders of magnitude larger than molecular and particle diffusivities due to Brownian motion. The depth of the turbulent boundary layer is related to the fetch (the distance traversed by the wind towards the forest across a uniformly rough surface). Over smooth areas such as beaches particle-sink mechanisms in operation are weak due to the absence of aerosol capturing elements.

The vertical wind profile within a canopy, in the interior of a forest when equilibration has occurred, can be described by for example a hyperbolic (Cowan 1968) or exponential formulation (cf. Wiman and Ågren 1985). However, the horizontal and vertical variations of

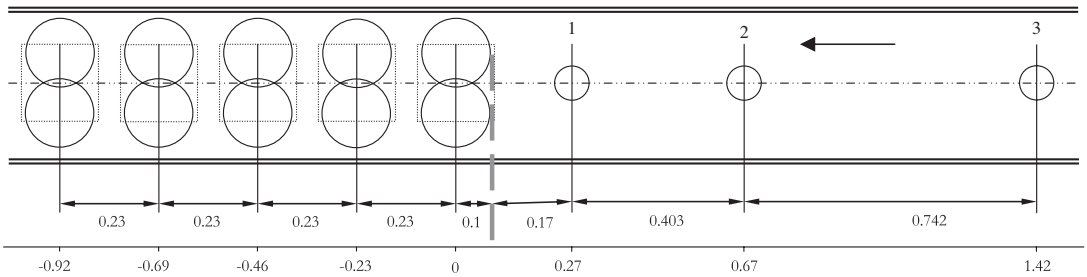

Fig. 1. Experimental arrangement, view from the top. The arrow indicates wind direction. The numbers above the plates indicate positions of the plates; number 3 indicates most upwind beach plate, thus with position closest to the aerosol source. The grey dashed line indicates position of the edge. We consider the edge to begin where the canopy begins; this varied between the runs by about 0.01 m.

the wind speed profile around a forest wall has a more complicated formulation (Wiman and Ågren 1985) inasmuch the roughness transition begins to affect the airflow well upwind of the edge and does not allow for equilibrated profiles until well downwind of the edge. The horizontal extension of the entire region of flow adjustment (from equilibrated profiles upwind of the edge to new, equilibrated, profiles downwind of it) is related to stand height and leaf area density, and is on the order of magnitude of five stand heights upwind and downwind (cf. Wiman and Ågren 1985). Edge effects are likely to be more pronounced for coniferous species than for deciduous ones (cf. Wuyts *et al*. 2008a) due to generally higher deposition velocities to coniferous species. This is because needles have dimensions small enough to make impaction a strong capture mechanism (Wiman and Ågren 1985). On the other hand, deciduous species with high trichome density and/or with sharp tips might well be equally efficient.

Although the basic principles that underpin edge deposition are beginning to be understood, many factors and processes remain to be further investigated. Wind-tunnel-based studies can offer important information to that end. Our study is based on the hypothesis that the effects of edge on the deposition processes would manifest themselves as increases in deposition rates both with respect to amounts deposited per unit ground surface area (as a result of the larger particle-collecting surface area that a canopy presents over a unit of ground surface area than does a flat plate) and with respect to amounts deposited per unit leaf area (as a result of the different particle-collecting characteristics that leaves would have in comparison with smooth plates, in addition to the different fluid dynamics around the edge vis-à-vis the smooth "beach"). In this contribution, we measure deposition rates with the primary objective of providing data on how they change across a transect from a smooth surface into an emulated 'forest'.

Methods and basic run conditions

Experimental design

Wind tunnels of various types are common in studies of the aerodynamics of, and aerosol deposition to, various vegetative collector arrangements (e.g. Wiman 1981, Kinnersley *et al*. 1994, Ould-Dada 2002, Reinap *et al*. 2009). The tunnel employed in our experiments is of a closed-circuit type and is described in Reinap *et al*. (2009). For the experiments reported in our present paper, we arranged a solid tunnel floor upwind of the forest model, which consisted of the leaf-arrangement support boxes. The distance between each of the rows in the forest aggregate was 0.23 m. The circular "beach plates" were placed upwind of the model forest, with the 1st, 2nd, and 3rd plates at 0.17 m, 0.57 m, and 1.32 m, respectively, from the edge (Fig. 1). Hence, in order to emulate the beach (i.e. for measuring deposition to a flat surface), these three plates (radius = 4 cm, thickness = 0.2 cm) were placed upwind on the tunnel floor at logarithmic distances counted from the forest edge. The plates were of the same type as the

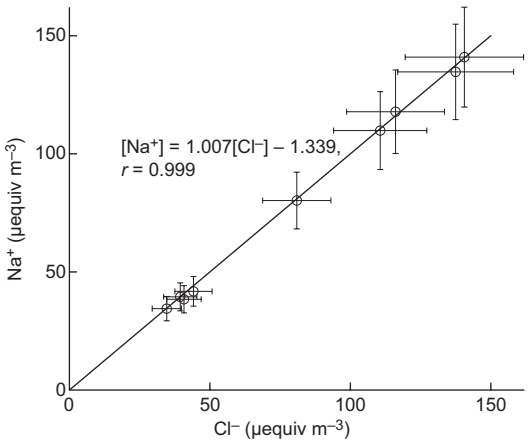

Fig. 2. Relationships between Cl^- and Na^+ in the tunnel air, in terms of concentration (μequiv m^{-3}) based on the impactor data. Solid line indicates the ideal relationship. The regression equation is given together with the correlation coefficient. Error bars indicate ±15% concentration values.

impactor plates, and thus smooth-surfaced and smooth-ended. For a pilot run only one square plate (6 × 6 cm, thickness 0.2 cm, and smooth-edged) emulating the beach was used and was placed at position 3.

Based on the considerations in the Theory section, our major hypothesis thus was that the effects of edge on deposition would be observable in this wind-tunnel environment. That hypothesis was first tested in a slightly simplified setup, namely with what we in the following call a "pilot run", and the result was sufficiently encouraging to suggest another nine runs. In designing our experiments we also hypothesized that (i) a difference with respect to aerosol-capture efficiency would be observable between cultivated samples and field samples, (ii) run conditions with high aerosol concentrations in the wind tunnel would generate different deposition rates than would low-concentration conditions, and (iii) "high" conditions would generate a mass-*versus*-particle-size distribution sufficiently different from the distribution generated under "low" conditions to enable us to study the effect of size-distribution characteristics on deposition.

In designing the experiments, we aimed to produce a relatively large fraction of coarse particles so as to emulate a coastal environment. Thus, the aerosol was generated by a modified bubble-bursting process in a retort; for the experiments addressed here, the retort was placed inside the tunnel. The retort contained a saturated 36% (by volume) sea salt solution, whereof ≥ 99.8% is NaCl. The equivalent Na^+/Cl^- ratio is thus essentially 1, and this ratio was preserved (Fig. 2) in the wind-tunnel aerosol which was iso-kinetically sampled with an Andersen cascade impactor (Thermo Electron Corporation) operating with a flow rate of 28.3 l min^{-1} and with 50% cut-off diameters (μm) from 9 down to 0.43; for details *see* Reinap *et al*. (2009). We focus on two tracers: chloride and sodium. Chloride is suitable for canopy exposure studies (e.g. Hansen and Nielsen 1998, Reinap *et al*. 2009) although, in the field, problems with leaching can occur in particular from autumn leaves (e.g. Staelens *et al*. 2008). Sodium, although not inert at leaf surfaces and thus potentially posing problems in exposure-and-wash-off studies, is also of interest as a tracer if interpretations are made with some caution (cf. Reinap *et al*. 2010).

The flow rate of the air jet injected through a nozzle (outlet diameter 1 mm) onto the surface of the sea-salt solution to "burst" it was controlled with a flowmeter (TSI 6330). Two flow rates were used, 16 l min^{-1} and 25 l min^{-1}. Wind speed in the tunnel was controlled through an electronic wind-generator regulator, and was measured with an air velocity transducer (TSI Model 8455-300). Average temperature and relative humidity at exposure was 23 °C and 60%, respectively. Additional details on the instrumentation employed in the wind tunnel are given in Reinap *et al*. (2009).

In our experiments, we used branches from laboratory-cultivated oaks and also oak-branches from the field. Oak seedlings (*Quercus robur*) were cultivated under controlled laboratory conditions with 12 hours of daylight at 20 °C. Field oak branches were picked from a three-years old oak forest stand (about the same age as the cultivated oak seedlings). The age of the seedlings may influence morphological leaf properties (firmness, hairiness, size and shape; cf. e.g., Lee *et al*. 1999). Leaves from the cultivated seedlings subjected to aerosol exposure were about 24 weeks old. However, some morphology characteristics of the leaves from field oaks might be dependent on the age of the leaves themselves

and also on the age of the tree from which the leaves are collected (cf. Lee *et al*. 1999). Well-leafed branches from cultivated and field oaks were washed for 10 minutes in a vessel containing 400 ml 18.2 MΩ cm^{-2} Milli-Q™ water (pre-exposure wash-off step). Branches were then left to dry in a clean-air environment, and then inserted into the wind tunnel with leaves arranged in five rows to build a model forest. The leaves of cultivated oaks were on the average (mean ± SD, $n = 50$) 9.0 ± 2.5 cm long and 5.0 ± 1.6 cm wide, while leaves from the field were on the average 11 ± 1.5 cm long and 5.0 ± 0.9 cm wide. A *t*-test showed no statistically significant difference ($p > 0.05$) between deposited amounts of substances from cultivated and field oak leaves. However, variation in size within the group of the cultivated oak leaves was greater, and they differed somewhat in shape (longer and more spiky tops) as compared with field oak leaves.

A commercially available system (PluggBoxes) was employed to implement the arrangement. On the average, over the ten separate runs, the total single-sided leaf areas of the leaf arrangement (A_{leaf}) were around 0.06 m^2 per row, and 0.21 m^2 per total model forest. There was no significant difference (*t*-test: $p > 0.05$) in leaf area per total model-forest aggregate between cultivated (0.22 ± 0.06 m^2) and field oaks (0.20 ± 0.03 m^2). A_{leaf} was determined from high-resolution photos of the leaves placed flat-down on a sheet of paper, with a help of digital surface-area quantification based on GIS and the Matlab software. LAI was here defined as leaf area per box (PluggBoxes) area (0.036 m^2) and ranged between 0.5 and 2 for cultivated oaks, with an average of 1.2 ± 0.4 (mean ± SD, $n = 30$), and between 0.8 and 1.4 for field oaks, with an average of 1.1 ± 0.2 (mean ± SD, $n = 20$). For the entire forest aggregate, i.e., the five rows, the total leaf area above the total PluggBox area (0.18 m^2) was 0.21 ± 0.05 m^2; i.e., the Leaf Area Index of the aggregate was 1.15 ± 0.26 m^2 m^{-2}.

As stated above, it is of interest to investigate potential differences between cultivated oaks and oaks from the field vis-à-vis deposition patterns along the transition region, to explore run conditions with low as well as high aerosol concentrations in the tunnel, and also to explore whether the "low" and "high" concentration conditions would generate different particle-size distributions. The structural design of our experiments therefore was as follows: four runs (including the pilot run) were performed with high aerosol concentrations ("high") and the model forest consisting of leafed branches from cultivated oaks ("cultivated"); two runs were with low aerosol concentrations ("low") and "cultivated"; two runs were with "high" and the model forest consisting of leafed branches from field oaks ("field"); two runs were with "low" and "field". The "high" and "low" concentration conditions were arranged through varying the flow rate of the air jet in the aerosol generator. In each of these runs, the model forest and the "beach" plates were exposed to the aerosol flux for 4 hours and with the wind speed set to 2 m s^{-1} as measured 0.35 m upwind of the model forest. High/low aerosol-concentration conditions therefore correspond to high/low exposure conditions.

A tendency towards slightly higher coarse-to-total ratios in the wind tunnel aerosol was found at low air-jet flow (16 l min^{-1}). During the low-concentration runs, the ratio coarse-to-total aerosol mass concentration (concentration of mass borne by coarse particles (> ca. 2 μm) relative to total mass concentration) was 0.33 for Cl^- and Na^+. At high exposure, the coarse-to-total ratio was 0.27 for both tracers. Log-normal curve fits showed that D_{pg} (the mean geometric particle size of the log-normal distribution) was on the average 1.5 μm and 1.8 μm, and σ_g (the geometric standard deviation of the distribution) 2.35 and 2.05, for the "high" and "low" conditions, respectively. However, no significant difference (*t*-test) could be established either between the D_{pg} values of to the high and low exposure conditions, or between the corresponding σ_g values. Therefore, in our further discussion we will focus on the particle size distribution averaged over all ten runs.

Exposure and wash-off principles

The pre-washed leaf arrangements (as described above) were inserted into the wind tunnel (cf. Fig. 1) and then exposed to the aerosol over the period of 4 hours which was found suitable after many previous tests run in order to optimize the

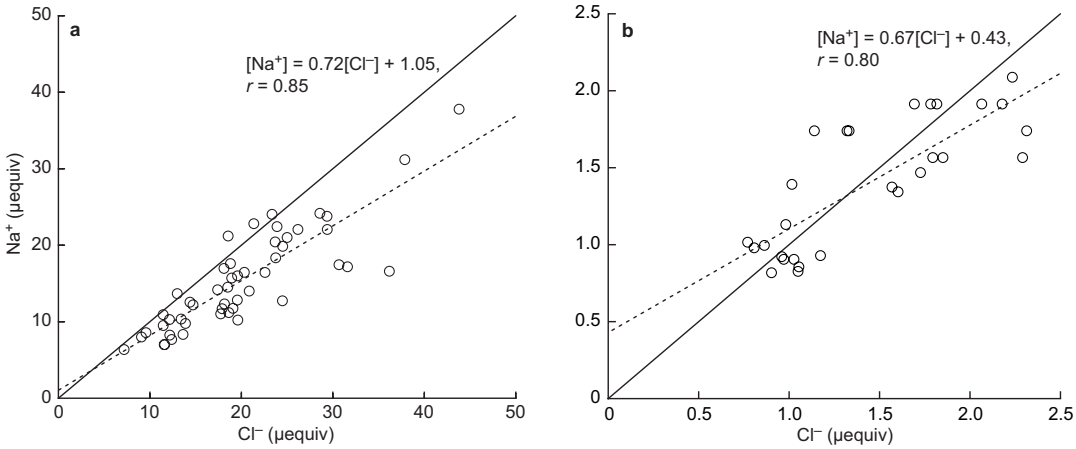

Fig. 3. Relationships between Cl^- and Na^+ in the wash-offs from (**a**) oak leaves and (**b**) "beach" plates, for all data.

experimental design (cf. Reinap *et al*. 2009). The exposed branches were kept under slow, automated shaking in a vessel for 20 min, the vessel initially containing 400 ml 18.2 MΩ cm^{-2} Milli-QTM water. After 5, 10 and 20 min, 30 ml of the solute was taken for the analysis; three sampling steps were thus used (*see* Reinap *et al*. 2009, and for in-depth descriptions Reinap *et al*. 2010). Each of the exposed "beach" plates and impactor plates was washed in 40 ml of 18.2 MΩ cm^{-2} Milli-QTM water for 20 min under slow, automated shaking. The solutes were then analyzed for chloride Cl^- and sodium Na^+ with Ion Selective Electrodes (ISE Orion 9617 and ISE Orion 8611) connected to an ISE meter Orion 720 Aplus. Blank impactor backup filter (final impactor stage) analysis showed a slight background content for Cl^- and Na^+; these contents (123 μg and 142 μg per filter, respectively) were corrected for in the final calculations of the size distributions.

Generated aerosol essentially contained the Na/Cl proportion inherent in the aerosol-generator solution (Fig. 2). The relationship between Cl^- and Na^+ in the wash-off solutes comes close to the equivalent Na^+/Cl^- ratio in the aerosol (Fig. 3). However, a deviation from the 1:1 ratio occurs, and is expected for the leaf wash-offs, because the leaves to some extent retain Na^+ (Reinap *et al*. 2010). We also found that the analytical uncertainty for each impactor stage was less than 5%. The total aerosol concentration, calculated as the sum over the impactor stages, was associated with an error of less than 15%, based on the square root of the sum of the squared errors per stage. The uncertainty in the washed-off amounts from leaves was calculated to be 5%. However, at lower concentrations (Fig. 3b), uncertainties increased towards 15%, so that the relationship between Cl^- and Na^+ in the wash-offs from the beach plates becomes less certain, albeit close to the equivalent Na^+/Cl^- ratio in the aerosol. For details on our uncertainty-estimation technique *see* Reinap *et al*. (2009, 2010). These uncertainty values can be used to estimate the overall uncertainty of data points representing averages of deposition rate; details of the procedures involved are given in the Results. Due to the above, we present the results on Cl^- and Na^+ separately.

Wind characteristics

The effects of wind speed on deposition rates and the leaves' aerosol-collection efficiency are of concern. The two-dimensional wind-velocity profile just upwind (ca. 0.35 m) of the exposed leaf arrangement was determined through measurements in the wind-tunnel space along vertical as well as horizontal coordinates, and was the average of three measurements for the setup used here with central tunnel-axis wind velocity set to 2 m s^{-1} (Fig. 4). Measurements were confined to the cross-section area extending a distance Δz from the tunnel floor and a distance Δy from the

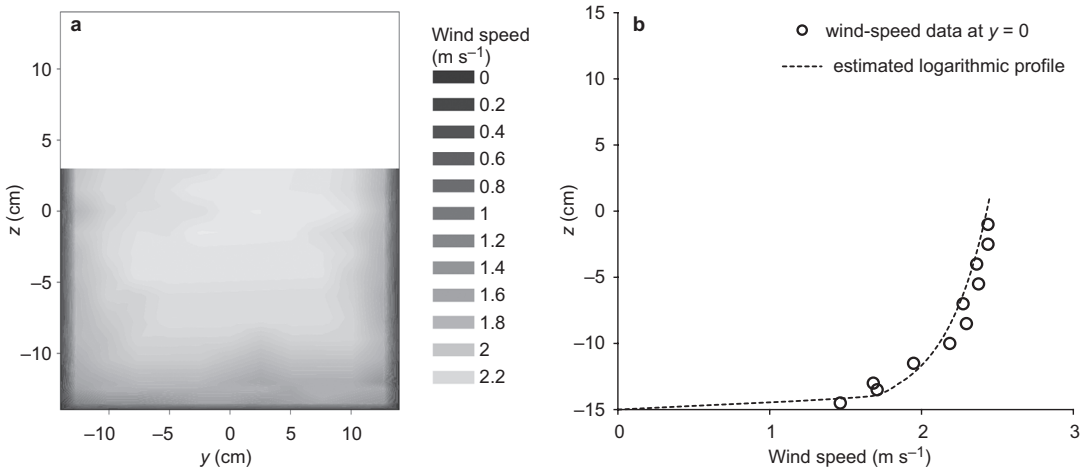

Fig. 4. (**a**) Wind speed as a function of y (width) and z (height) coordinates in the tunnel 0.35 m upwind the model oak forest for wind velocities 2 m s^{-1} at the tunnel axis (y = 0, z = 0). The white area represents space not accessible to measurements. (**b**) Wind speed as a function of z at y = 0. The dashed curve represents the logarithmic profile modelled from the measured data, with u^* = 0.12 m s^{-1} and z_o = 0.00003 m; zero-plane displacement d is assumed to be negligible.

walls and upwards to the level of 14 cm above the tunnel floor; the remaining area was not accessible to measurements. For the wind-speed measurements, the sensor dimensions allowed for $\Delta z \approx 0.5$ cm and $\Delta y \approx 1$ cm. The approaching wind profile was of a logarithmic type from the tunnel floor and upwards towards the central axis of the tunnel (Fig. 4b), declining towards the tunnel walls (Fig. 4a); for symmetry reasons it should do so also towards the tunnel ceiling.

Because of contamination risks, measurements of wind profiles inside the "forest models" could not be carried out concomitantly with runs during which the "forests" were exposed to an aerosol flux. However, in test runs it was possible to measure wind profiles inside the canopy. For vertical wind profiles without and with a "forest model" present, the wind velocity was 5 m s^{-1} at the tunnel central axis and at the position for the iso-kinetic aerosol-sampling probe inlet (Fig. 5). The height of the "forest model" was about 0.12 m, its lower canopy level around 0.065 m above the tunnel floor, and its LAI (single-sided) about 2.8.

Without a "forest model" the profile is approximately logarithmic up to $z \approx 0.15$ m, but, as expected, adopts a more complicated shape inside the forest model (Fig. 5). This profile shape, with a velocity increase (a "bulge") below the lower canopy limit and the ground (the "trunk space"), is not uncommon in field situations (cf. e.g., Gardiner 1994). In the "trunk region", there is thus a counter-gradient momentum flux presenting a resistance to downward particle movement. This means that deposition rather occurs in the canopy than to the tunnel floor.

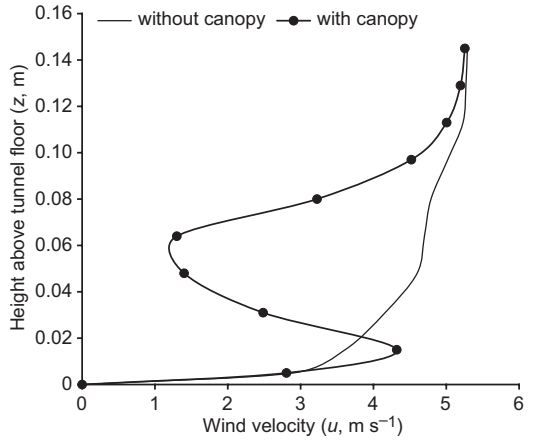

Fig. 5. Wind profiles measured with and without "forest model" in the tunnel.

A common approach is to interpret the relation between the mean wind profile and turbulence as a set of eddies with extensions given by

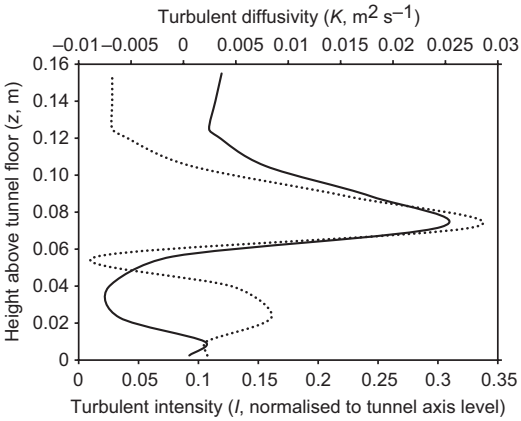

Fig. 6. Turbulence inside (< 0.12 m) and above the "mini-forest" in terms of eddy diffusivity (solid line) and turbulent intensity (dashed line), calculated from the data in Fig. 5.

a so-called mixing length, L_{mix} (cf. e.g., Monteith and Unsworth 1990). One can then define the turbulent eddy diffusivity $K(z)$ as (cf. Wiman and Ågren 1985)

$$K(z) = [L_{mix}(z)]^2[du(z)/dz]S(z) \qquad (1)$$

where $u(z)$ is the mean wind profile, and $S(z)$ is a function that describes effects of air stability conditions; $S(z) = 1$ under neutral conditions, which were at hand in our experiments.

Above (or outside) the forest, L_{mix} is given by $L_{mix}(z) = k(z - d)$, where k is von Karman's constant (= 0.41) and d is the zero plane displacement.

Following Wiman and Ågren (1985) and Wiman (1985), L_{mix} inside the forest can be written as

$$L_{mix}(z) = k\frac{1-\exp\left(\frac{-zq\mathrm{LAI}_2}{z_c}\right)}{q\mathrm{LAI}_2/z_c} \qquad (2)$$

where LAI_2 is the double-sided leaf area index, z_c is the canopy height, and q is a factor relating to the orientation of the leaves in the airflow. For our purposes here, the value of q is not critical and can be set to 2.

The term $du(z)/dz$ can be estimated from the data (*see* Fig. 6) in various ways, the simplest of which is to calculate $(u_{j+1} - u_j)/(z_{j+1} - z_j)$ for the various strata j in the within-canopy data sequence. Above the forest, $K(z) = ku^*(z - d)$, and with the common assumption that $d \approx 0.7z_c$ and u^* can be estimated from the data. The turbulent eddy diffusivity (pertaining to what is shown in Fig. 5) can then be calculated (*see* solid line in Fig. 6). Among other things, the K profile in Fig. 6 highlights the counter-gradient momentum flux in the "trunk region".

The mixing length is also related to velocity fluctuations u' and w', and in the isotropic case one can write $u' = w' = L_{mix}(z)[du(z)/dz]$. Equation 3 can then be used to represent turbulence also in terms of turbulent intensity $I(z)$ (*see* doted line in Fig 6):

$$I(z) = (u'w')^{0.5}/\bar{u} \qquad (3)$$

with $\bar{u}$ being the mean wind speed at the tunnel axis. The occurrence of a maximum in turbulence intensity within the forest model suggests, again, that significant parts of the deposition are at the canopy level. The intensity profile is in a reasonable agreement with profiles obtained for "forest models" in much larger wind tunnels (*see* e.g. Meroney 1968, Kinnersley *et al*. 1994) wherein turbulence similar to that occurring in real forests was generated (cf. Raupach and Thom 1981, Finnigan and Shaw 2000).

Size distributions

The particle size distribution of sodium and chloride was averaged over all ten runs, and concentration per Δln interval was normalized to total chloride and sodium concentrations *versus* particle diameter. The respective distributions overlap perfectly (Fig. 7). A log-normal distribution was, therefore, fitted to all the data (chloride plus sodium). Calculations for modelled data reported here were based on the formula for a log-normal distribution by adjusting the geometric standard deviation and geometric mean particle size according to different particle size modes. Calculations of the coarse-particle (diameter > 2 μm) to total mass ratio show that the distribution of the aerosol-borne mass of chloride and sodium is fine-particle oriented. On average, 70% of the chloride as well as sodium mass is carried by fine particles (diameter < 2 μm).

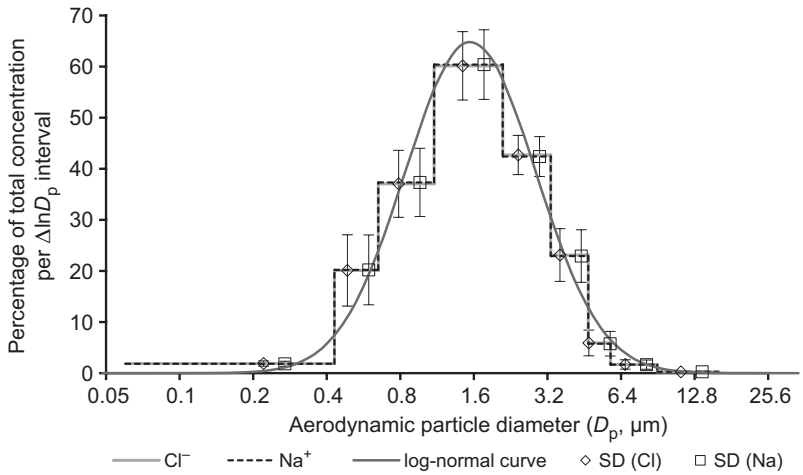

Fig. 7. Distributions of average aerosol particle mass-concentration *versus* aerodynamic particle size for all runs for chloride and sodium. The mean geometric particle size is on average 1.55 μm, and the geometric standard deviation is approximately 1.85. The correlation coefficient (r) for the modelled *versus* measured data is 0.99. The upper end limit of particle diameter was set to 16 μm (a reasonable limiting size; cf. e.g., Foltescu *et al.* 2005) and the lower limit to 0.06 μm (a reasonable limiting size for natural aerosol particles).

Results

Introductory observations

An overview of the run conditions and results is given in the Appendix. Our overarching hypothesis addressed the extent to which deposition patterns along the beach-forest edge-forest interior would be observable and quantifiable; we return to that in the next section. First, however, we found that our hypothesis that a difference with respect to aerosol capture-efficiencies of cultivated and field samples was not confirmed. This result was obtained after estimating uncertainties in each individual respective "forest" data value from first differentiating, for each value contributing to the data point i, the relationship

$$D_i = M_{\mathrm{leaf},i}/(A_{\mathrm{g},i}\tau_i),$$

where D_i is the deposition rate, $M_{\mathrm{leaf},i}$ is the amount washed from the leaves in a certain row, $A_{\mathrm{g},i}$ is the ground surface area beneath the leaves (in our study, the PluggBox area) or the leaf surface area, and τ_i is the exposure duration. Evaluating the partial errors gives a resulting uncertainty dD_i/D_i around ±5%. Then, with for instance three data values (D_1, D_2, D_3) constituting a "forest" data point for the deposition rate D (for example, the three runs with cultivated samples under high concentrations), an overall estimate can be obtained from

$$dD/D = [(dD_1/D_1)^2 + (dD_2/D_2)^2 + (dD_3/D_3)^2]^{0.5}.$$

This results in an uncertainty per "forest" data point around ±10%. For the beach plates analogous considerations can be made; however, since low or very low concentrations were at hand in this case in the solute subject to ISE analysis, each "beach" data value is associated with an uncertainty around ±25%.

Next, the hypothesis that high aerosol concentrations would generate different deposition rates than would low concentrations was explored. Regression analysis of our data indicated that the beach-plate and model-forest deposition rates of chloride increased linearly with the aerosol concentration (beach-plate deposition $r = 0.81$ and model-forest deposition $r = 0.87$, $p < 0.01$), within the concentration range studied.

We also hypothesised that mass-*versus*-particle-size distributions generated under "high" and "low" conditions would differ sufficiently to enable us to study the effect of size-distribution characteristics on deposition. As already stated (*see* "Size distributions"), that hypothesis was not confirmed.

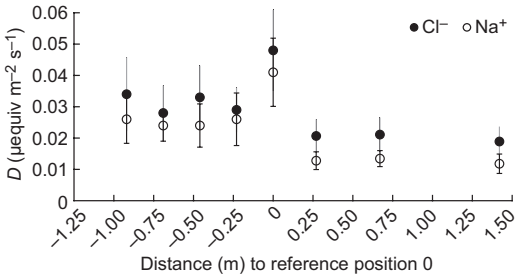

Fig. 8. Average deposition rates (*D*) of the ten runs, in terms of deposited amounts per unit time and ground surface area, for Cl^- and Na^+ as a function of distance upwind from the model forest edge, towards the edge, farther downwind into the forest interior, and then towards the forest end edge. In the figure, wind direction is from right to left. Data points at positions upwind of the edge pertain to "beach" plates. Reference position 0 is given in Fig. 1. Error bars are 95% confidence intervals.

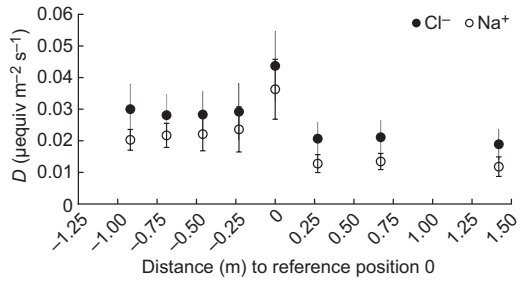

Fig. 9. Average deposition rates (*D*) of the ten runs, in terms of deposited amounts per unit time and leaf/collector surface area, for Cl^- and Na^+ as a function of distance upwind from model forest edge, towards the edge, farther downwind into the forest interior, and then towards the forest and edge. In the figure, wind direction is from right to left. Data points at positions upwind of the edge pertain to "beach" plates. Reference position 0 is given in Fig. 1. Error bars are 95% confidence intervals.

Deposition rates

For the wind speed of 2 m s^{-1}, there was a clear longitudinal deposition pattern along the beach-forest edge-forest interior (Figs. 8 and 9).

Since the deposition rates were non-normally distributed, to test the significance of the differences we used a Mann-Whitney test. The deposition rate per ground area to the first row was significantly higher than to the remaining rows (Mann-Whtiney: $Z = 2.69$, $p = 0.0071$ for Cl^-; $Z = 3.02$, $p = 0.0025$ for Na^+; in both cases for $n_{edge} = 10$, $n_{interior} = 40$), the enhancement factor was between 1.5 (Cl^-) and 1.6 (Na^+). There was a tendency (although not statistically significant) towards the increase also at the downwind edge. The deposition rate per ground area to the first row was significantly higher than to the beach plates (Mann-Whtiney: $Z = 4.18$, $p < 0.0001$ for Cl^-; $Z = 4.64$, $p < 0.0001$ for Na^+; in both cases for $n_{edge} = 10$, $n_{beach} = 28$), the enhancement factor being between 2.4 (Cl^-) and 3.2 (Na^+).

Deposition rates in relation to leaf (rather than ground) surface area add some information on the leaves' efficiencies in capturing particles (and thus V_L, deposition velocity per unit leaf area; cf. Wiman and Ågren 1985) which is not obvious in the previous deposition-rate concept. We found that the deposition rates in relation to leaf surface area follow a pattern similar to that related to deposition per ground surface area (Fig. 9).

The deposition rate per collector (leaf) area to the first row was significantly higher than to the remaining rows (Mann-Whtiney: $Z = 2.55$, $p = 0.011$ for Cl^-; $Z = 3.23$, $p = 0.0013$ for Na^+; in both cases for $n_{edge} = 10$, $n_{interior} = 40$), the enhancement factor being between 1.5 (Cl^-) and 1.7 (Na^+). In this case, the tendency for the Cl^- increase also at the downwind edge is not reflected in the Na^+ data. The deposition rate per collector area to the first row was significantly higher than to the beach plates (Mann-Whtiney: $Z = 3.88$, $p = 0.0001$ for Cl^-; $Z = 4.62$, $p < 0.0001$ for Na^+; in both cases for $n_{edge} = 10$, $n_{beach} = 28$), the enhancement factor being between 2.2 (Cl^-) and 2.9 (Na^+).

Discussion

Introductory observations

The forest-wall effect should only be noticeable over a distance of about five times the canopy height downwind of the edge (cf. Wiman and Ågren 1985, Erisman *et al*. 2003). We have a model forest that is on the average 0.12 m high, 0.25 m wide and 1.22 m long. The estimated fetch distance ranges up to 0.75 m upwind of the forest edge (cf. Monteith and Unsworth 1990). Our results demonstrate the effects of edge on the deposition. The increase in deposition rates

at the edge was most pronounced in relation to the beach, whereas — in comparison with that observation — there was a moderate increase in the interior of the forest relative to the beach. This finding is consistent with Ould-Dada *et al*. (2002), and also has a theoretical explanation. As the air flow begins to equilibrate after the edge, major effects of the edge begin to fade, making the aerodynamic part of the aerosol-sink mechanisms somewhat more similar to those along the beach. Also, wind speeds inside the canopy are low (Fig. 5) resulting in subsequently low particle-capture efficiencies. That, in turn, leads to lower deposition rates at "down-edge fetch" distance (up to row 4, 0.75 m) followed by a tendency towards the edge effect also downwind at the end of the forest. This finding is consistent with the modelling results presented by Wiman and Ågren (1985). The edge effect downwind at the end of the forest is mainly due to growing turbulent exchange as a new roughness transition begins, albeit here from rough to smoother aerodynamics (cf. De Schrijver *et al*. 1998, Gash *et al*. 1986, Pahl 2000).

Previous studies (Gardiner 1994, Kinnersley *et al*. 1994, Wuyts *et al*. 2008a, 2008b) revealed that wind speed is typically smaller within the canopy than at the canopy top. Although the velocity pattern is quite complex over the first part of the transition (Wiman and Ågren 1985), wind velocity decreases roughly exponentially with increasing distance from the edge. Turbulence also shows complexities within a canopy interior (*see* Figs. 5 and 6) and, among other things, is linked to leaf fluttering (*see* also Raupach and Thom 1981, Arya 1988, Dupont and Brunet 2008). Sparse forests might experience higher wind speeds within the canopy than a dense forest (Gardiner *et al*. 1997), and this is thus an additional example of factors that require further research.

From the model studies, Wiman and Ågren (1985) showed that the higher wind speed at the forest edge, as compared with that in the interior, was among the factors that increased the dry deposition of particles; these and related findings were indirectly supported by field measurements of horizontal aerosol-concentration profiles across aerodynamic roughness transitions from open areas and into a forest (Wiman and Lannefors 1985, Wiman *et al*. 1985). Moreover, dry deposition was found to be governed to the greatest extent by particle size. In the model by Wiman and Ågren (1985), the size-distribution changes over the transition from the forest edge towards the forest interior. This is because across the forest edge larger particles become depleted; thus gravitational settling and impaction become less important as the aerosol moves through the forest. Particles in the size range from ca. 0.1 to 1 μm are subject to almost negligible depletion, whereas the deposition of very small (< ca. 0.1 μm) particles would become significant because of Brownian diffusion across air-flow streamlines. For fine particles (in our case, particles with diameters < 2 μm) the behaviour inside the forest is mainly governed by turbulent exchange and in-canopy wind velocity. In the model case, however, the aerosol is at the same time replenished by continuous vertical influx at the canopy top, so that sinks (depletion to due to inside-forest deposition) and sources (replenishment from above-forest aerosol) tend towards equilibration. Similar tendencies towards concentration equilibrium would be at hand in our forest aggregate.

We found a minor difference in deposition-rate quantities between our tracers (*see* Fig. 4) which is likely to reflect retention of sodium at the leaf surface (cf. Reinap *et al*. 2010). In essence, however, deposition rates of both tracers showed similar patterns with a maximum around the forest edge.

There were no significant differences in terms of dimensions and leaf area between cultivated oaks and field oaks. However, field oaks could have different morphological properties in regard to firmness and hairiness, but to investigate these differences would require micro-scale analysis that is beyond the scope of this paper. Interestingly, however, if such micro-scale differences existed between our leaves from cultivated oaks and the field-oak leaves, the effects of these characteristics on aerosol-particle capture efficiency were too small to express themselves in relation to the effects on efficiency that emanate from the macro-scale features of *Quercus robur* leaves (dimensions, overall geometry and shape). Also, the inter-leaf differences seem to have been small enough to generate relatively moderate variation in deposition velocities, although the

larger variation (e.g. deposited amounts, *see* the Appendix) in the field-oak deposition data than in the cultivated-oak deposition data is consistent with some of our previous studies (Reinap *et al*. 2008). Clearly, potential implications of leaf micro-morphology need further study.

Comparisons with other studies

Many of the previous edge-effects studies (Draaijers 1993, Ould-Dada *et al*. 2002, Wuyts *et al*. 2008a, 2008b) focused on coniferous species whereas research on deciduous forests is underrepresented; however, some studies with focus on beech stands and other deciduous species exist (Devlaeminck *et al*. 2005, Wuyts *et al*. 2008b, Weathers *et al*. 2001, Balsberg-Påhlsson and Bergkvist 1995). Although, to our knowledge, there are no wind-tunnel-based studies quantifying deposition rates for oak forest edges, some qualitative comparisons can be made. Our observations of enhanced deposition of aerosol particles at the model-forest wall are in qualitative agreement with findings of several other studies on edge effects. Using throughfall technique, Wuyts *et al*. (2008b) found that deposition at forest edges was clearly enhanced in comparison with that in the forest interior, pointing out that the chloride ion showed the most pronounced edge effect. A study by Draaijers (1993) revealed that net throughfall fluxes inside forests increase exponentially towards forest edges, where the most pronounced edge effect was observed for Na, Cl and Mg as a result of dry deposition of super-micron sea-salt particles. For these elements, a strong correlation with leaf area density was found, as a result of in-canopy wind speeds that basically determine the differences between forest edge and forest interior dry deposition (Erisman *et al*. 2003). Beier and Gundersen (1992) found that Na^+ and Cl^- substances deposited as particles showed the most pronounced Norway spruce edge effect as compared with the edge effect of gaseous substances (cf. also Draaijers 1993, Spangenberg and Kölling 2004, Wuyts *et al*. 2008c). Edge-enhancement factors reported in the literature show a very wide range. For instance, Balsberg-Påhlsson and Bergkvist (1995) reported the enhancement factors of 1.6 for SO_4-S and 2.4 for inorganic N, whereas De Schrijver *et al*. (1998) found enhancement factors around 2 for NH_4^+-N, and Wuyts *et al*. (2006) cited the data that suggest cases with enhancement factors up to around 4. However, in the field, forest edges are exposed to a much more complex combination of factors than in our controlled experiments (aerosol with a known mass-*versus*-particle size distribution, stable and controlled wind-velocity conditions and LAI parameters). Also, in the field, aerosol-borne compounds have very different particle-size distributions. Throughfall measurements in the field also involve effects of gaseous, fog, and wet deposition and involve other effects in the edge region (e.g. enhanced effects of drought situations). In addition, coniferous forests and deciduous forests operate quite differently as aerosol sinks, thus conducive to a broad range in empirical edge-effect values.

In order to facilitate comparisons with studies that address deposition velocities instead of deposition rates, we note that our results in some respects can be translated into capture efficiencies, deposition velocities related to unit leaf area, and deposition velocities related to ground surface area (V_g); details on such transformations are given in Reinap *et al*. (2009). In our current contribution, we focused on V_g. In order to estimate V_g, we assume that aerosol particles were carried towards the edge by essentially the same wind velocity of 2 m s^{-1} over the major part of the cross-section area of the tunnel, so that in the region occupied by the leaves in the first row the flux profile is essentially flat. This simplification is reasonable (Reinap *et al*. 2009; cf. also Fig. 5) for the first row, i.e., the edge region, so that V_g can be estimated by dividing the deposition rate to the first row by the aerosol-borne concentration of the tracers (Cl^- and Na^+). This gives a V_g (mean over all runs ± 95%CI) in the edge region of 0.063 ± 0.011 cm s^{-1} for Cl^- and 0.056 ± 0.013 cm s^{-1} for Na^+. These values, if transformed to deposition velocities per unit leaf area, are consistent with those found by Reinap *et al*. (2009) for oak leaves, but somewhat higher; a result that can be explained by the somewhat more coarse-particle oriented size distribution used in the present study. For the beach plates, the mean values of V_g are 0.028 ± 0.004 cm s^{-1} for Cl^- and 0.018 ± 0.003 cm s^{-1} for Na^+.

Our experiment demonstrates and helps explain the effects of edge on deposition, and quantifies these effects in a wind-tunnel environment. Scaling-up procedures to emulate real forest stands need to be based on fairly advanced modelling such as exemplified in Wiman and Ågren (1985) and on access to information on specifics of the field situation of interest, among them wind-velocity profiles and stand-structure characteristics (leaf-area density distributions, LAI, canopy height, and spacing between trees). Our data confirm the notion that field measurements of deposition in the interior of a forest "island" in an otherwise open landscape would underestimate the deposition to the entire forest (cf. e.g. Wiman and Ågren 1985, De Schrijver *et al*. 2007). Approximate calculations suggest that the edge effect would cause an increase of only a few percent for a stand with an extension of around 5 km, and deposition information based on, for instance, moss or throughfall studies in the interior of the forest would then be reasonably representative. However, for a stand extension of about 0.5 km, such information might well underestimate the deposition to the entire stand by about 20%–30%. For a landscape fragmented into many stands of that extension, or smaller, generalisations to the entire landscape — were they based on measurements in stand interiors only — might result in a substantial underestimation.

Conclusions and implications

Our data demonstrate the enhanced deposition at a forest edge. The deposition rate around the forest edge was 2–3 times higher than to the beach and 50%–60% higher than to the interior of the forest. The deposition velocity at the edge was 0.06 cm s^{-1}, which is 2–3 times higher than the beach-deposition velocity. The results are in reasonable agreement with those obtained from deposition models (cf. e.g., Pryor *et al*. 2008), previous wind-tunnel investigations (e.g. Ould-Dada *et al*. 2002), and field studies (e.g. Wuyts *et al*. 2008b). There was no significant difference between cultivated and field oaks with respect to deposition at the forest edge. Deposition rates of chloride and sodium show similar patterns with a maximum around the forest edge.

Patchiness, and thus edges, dominate our landscapes. Therefore, it is of great importance to study edge effects on deposition processes that involve pollutants as well as nutrients. In particular, coastal forest sites would experience enhanced levels of sea salt deposition as a result of strong on-shore winds that might result in high concentrations of sea-salt particles (Foltescu *et al*. 2005). In addition, patchiness in terms of landscape physiognomy needs to be seen in combination with special aerodynamics in complex terrain. For instance, wind circulation systems in coastal areas (land/sea breeze) imply that a marine aerosol can become transported many times towards (daytime) as well as out from (nighttime) forest edges (cf. e.g., Skakalova *et al*. 2003). Similar considerations can be made with respect to mountain-valley circulation of aerosols, and related effects on airflows in complex terrain (cf. e.g., Lindberg and Owens 1993). We also found that the size distribution in our experiments compares fairly well with those pertaining to natural marine aerosols (cf. Rinaldi *et al*. 2009).

In this contribution, we showed that a wind-tunnel approach is a good complementary method for investigating edge effects on deposition processes for tree species that have been recently under-represented. The results facilitate further estimates of aerosol-borne inputs of various substances to forests that would experience alteration due to climate change and shifts in forestry practices.

Acknowledgements: This work was funded by the Linnaeus University Faculty Board of Science and Engineering. Svenningsson thanks the Swedish Research Council for their funding. We are grateful to Lise Lotte Sørensen for valuable comments on the manuscript. Suggestions for improvements by two anonymous reviewers are greatly appreciated. Some of the instruments used for the experiments were part of the IEDA project, funded by the Swedish Research Council. We also thank Georg Gleffe, Anders Månsson, and Sven Bergh for assisting with adapting the wind-tunnel to the particular experiments involved in this study.

References

Arya S.P. 1988. *Introduction to micrometeorology*. Academic Press Inc., London.

Balsberg Påhlsson A.-M. & Bergkvist B. 1995. Acid deposi-

tion and soil acidification at a southwest facing edge of Norway spruce and European beech in south Sweden. *Ecol. Bull.* 44: 43–53.

Beier C., Gundersen P. & Rasmussen L. 1992. A new method for estimation of dry deposition of particles based on throughfall measurements in a forest edge. *Atmos. Environ.* 26A: 1553–1559.

Bodin P. & Wiman B.L.B. 2007. The usefulness of stability concepts in forest management when coping with increasing climate uncertainties. *Forest Ecol. Manage.* 242: 541–552.

Cowan I.R. 1968. Mass, heat and momentum exchange between stands of plants and their atmospheric environment. *Q. J. R. Meteor. Soc.* 94: 318–332.

De Schrijver A., Nachtergale L., Roskams P., De Keersmaekerb L., Sylvie Musschea S. & Lust N. 1998. Soil acidification along an ammonium deposition gradient in a Corsican pine stand in northern Belgium. *Environ. Pollut.* 102, Sl: 427–431.

De Schrijver A., Devlaeminck R., Mertens J., Wuyts K., Hermy M. & Verheyen K. 2007. On the importance of incorporating forest edge deposition for evaluating exceedance of critical pollutant loads. *Applied Vegetation Science* 10: 293–298.

Devlaeminck R., De Schrijver A. & Hermy M. 2005. Variation in throughfall deposition across a deciduous beech (*Fagus sylvatica* L.) forest edge in Flanders. *Sci. Total Environ.* 337: 241–252.

Draaijers G. 1993. *The variability of atmospheric deposition to forests: the effects of canopy structure and forest edges*. Ph.D. thesis, Department of Physical Geography, University of Utrecht, The Netherlands.

Draaijers G.P.J. & Erisman J.W. 1993. Atmospheric sulfur deposition onto forest stands: throughfall estimates compared to estimates from inference. *Atmos. Environ.* 27: 43–55.

Draaijers G.P.J., Van Ek R. & Bleuten W. 1994. Atmospheric deposition in complex forest landscapes. *Boundary-Layer Meteorol.* 69: 343–366.

Erisman J.W. & Draaijers G. 2003. Deposition to forests in Europe: most important factors influencing dry deposition and models used for generalisation. *Atmos. Pollut.* 124: 379–388.

Finnigan J.J. & Shaw R.H. 2000. A wind-tunnel study of airflow in waving wheat: an EOF analysis of the structure of large-eddy motion. *Boundary-Layer Meteorol.* 96: 211–255.

Foltescu V.L., Pryor S.C. & Bennet C. 2005. Sea salt generation, dispersion and removal on the regional scale. *Atmos. Environ.* 39: 2123–2133.

Fowler D., Pilegaard K., Sutton M. A., Ambus P., Raivonen M., Duyzer J., Simpson D., Fagerli H., Fuzzi S., Schjoerring J.K., Granier C., Neftel A., Isaksen I.S.A., Laj P., Maione M., Monks P.S. & Burkhardt J. 2009. Atmospheric composition change: ecosystems–atmosphere interactions. *Atmos. Environ.* 43: 5193–5267.

Gardiner B.A. 1994. Wind and wind forces in a plantation spruce forest. *Boundary-Layer Meteorol.* 67: 161–186.

Gardiner B.A., Stacey G.R., Belcher R.E. & Wood C.J. 1997. Field and wind tunnel assessments of the implications of respacing and thinning for tree stability. *Forestry* 70: 233–252.

Gash J.H.C. 1986. Observations of turbulence down-wind of a forest-heath interface. *Boundary-Layer Meteorol.* 36: 227–237.

Gustafsson M.E.R. & Franzén L.G. 2000. Inland transport of marine aerosol in southern Sweden. *Atmos. Environ.* 34: 313–325.

Hansen B. & Nielsen K.E. 1998. Comparison of acidic deposition to semi-natural ecosystems in Denmark — coastal heath, inland heath and oak wood. *Atmos. Environ.* 32: 1075–1086.

Hicks B.B., Matt D.R., McMillen R.T., Womack J.D., Wesely M.L., Hart R.L., Cook D.R., Lindberg S.E., de Pena R.G. & Thomson D.W. 1989. A field investigation of sulfate fluxes to deciduous forest. *J. Geophys. Res.* 94: 13003–13011.

Kinnersley R.P., Farrington-Smith J.G., Shaw G. & Minski M.J. 1994. Aerodynamic characterisation of model tree canopies in a wind tunnel. *Sci. Total Environ.* 157: 29–33.

Lee J.H., Hashizume H. & Kwon K.W. 1999. Morphological variations in leaves and foliar trichomes along with developmental age of four deciduous *Quercus* taxa. *Jour. Korean. For. Soc.* 88: 11–17.

Lindberg S.E. & Owens J.G. 1993. Throughfall studies of deposition to forest edges and gaps in montane ecosystems. *Biogeochemistry* 19: 173–194.

Meroney R.N. 1968. Characteristics of wind and turbulence in and above model forests. *J. Appl. Meteorol.* 7: 780–788.

Monteith J.L. & Unsworth M.H. 1990. *Principles of environmental physics*. Edward Arnold, London.

Ould-Dada Z. 2002. Dry deposition profile of small particles within a model spruce canopy. *Sci. Total Environ.* 286: 83–96.

Ould-Dada Z., Copplestone D., Toal M. & Shaw G. 2002. Effect of forest edges on deposition of radioactive aerosols. *Atmos. Environ.* 36: 5595–5606.

Pahl U. 2000. *Numerische Simulationen zum Einfluss von Waldbestandshomogenitäten auf die Windverhältnisse und die trockene Spurenstoffdeposition*. Ph.D. thesis, Institute of Meteorology and Climatology, Leibniz University of Hannover.

Pryor S.C., Gallagher M., Sievering H., Larsen S.E., Barthelmie R.J., Birsan F., Nemitz E., Rinne J., Kulmala M., Grönholm T., Taipale R. & Vesala T. 2008. A review of measurement and modelling results of particle atmosphere-surface exchange. *Tellus* 60B: 42–75.

Raupach M.R. & Thom A.S. 1981. Turbulence in and above plant canopies. *Ann. Rev. Fluid Mech.* 13: 97–129.

Reinap A., Wiman B.L.B. & Svenningsson B. 2008. Aerosol capture by oak leaves — an experimental investigation. In: *Proceedings of the 2008 European Aerosol Conference, Thessaloniki, Greece*, abstract T03A058P.

Reinap A., Wiman B.L.B., Svenningsson B. & Gunnarsson S. 2009. Oak leaves as aerosol collectors: relationships with wind velocity and particle size distribution. *Trees* 23: 1263–1274.

Reinap A., Wiman B.L.B., Gunnarsson S. & Svenningsson B. 2010: Dry deposition of NaCl aerosols: theory and

method for a modified leaf-washing technique. *Atmos. Meas. Tech. Discuss.* 3: 3851–3876.

Rinaldi M., Facchini M.C., Decesari S., Carbone C., Finessi E., Mircea M., Fuzzi S., Ceburnis D., Ehn M., Kulmala M., de Leeuw G. & O'Dowd C.D. 2009. On the representativeness of coastal aerosol studies to open ocean studies: Mace Head — a case study. *Atmos. Chem. Phys.* 9: 9635–9646.

Skakalova T.S., Savov P.B., Grigorov I.Y. & Kolev I.N. 2003. Lidar observation of breeze structure during the transition periods at the southern Bulgarian Black Sea coast. *Atmos. Environ.* 37: 299–311.

Skjøth C.A., Geels C., Hvidberg M., Hertel O., Brandt J., Frohn L.M., Hansen K.M., Hedegård G.B., Christensen J.H. & Moseholm L. 2008. An inventory of tree species in Europe — an essential data input for air pollution modelling. *Ecol. Modell.* 217: 292–304.

Solomon S., Qin D., Manning M., Chen Z., Marquis M., Averyt K.B., Tignor M. & Miller H.L. (eds.) 2007. *IPCC 4th Assessment Report*. Cambridge University Press, Cambridge, United Kingdom and New York, NY, USA.

Spangenberg A. & Kölling C. 2004. Nitrogen deposition and nitrate leaching at forest edges exposed to high ammonia emissions in southern Bavaria. *Water Air Soil Pollut.* 34: 233–255.

Staelens J., Houle D., De Schrijver A., Neirynck J. & Verheyen K. 2008. Calculating dry deposition and canopy exchange with the Canopy Budget Model: review of assumptions and application to two deciduous forests. *Water Air Soil Pollut.* 191:149–169.

Weathers K.C., Cadenasso M.L. & Pickett S.T.A. 2001. Forest edges as nutrient and pollutant concentrators: potential synergisms between fragmentation, forest canopies, and the atmosphere. *Conserv. Biol.* 15: 1506–1514.

Wiman B.L.B. 1981. Aerosol collection by Scots pine seedlings: design and application of a wind tunnel method. *Oikos* 36: 83–92.

Wiman B.L.B. & Ågren G.I. 1985. Aerosol depletion and deposition in forests — a model analysis. *Atmos. Environ.* 19: 335–347.

Wiman B.L.B. & Lannefors H.O. 1985. Aerosol characteristics in a mature coniferous forest — methodology, composition, sources and spatial concentration variations. *Atmos. Environ.* 19: 342–362.

Wiman B.L.B., Ågren G.I. & Lannefors H.O. 1985. Aerosol concentration profiles within a mature coniferous forest — model *versus* field results. *Atmos. Environ.* 19: 363–367.

Wiman B.L.B., Velchev K., Gaydarova P.N., Donev E.H. & Yurukova L. 2003. A note on aerosol mass-versus-size distributions in the south-east Bulgarian Black Sea coastal region. *Bulg. J. Meteorol. Hydrol.* 13: 26–39.

Wuyts K., Verheyen K., De Schrijver A., Cornelis W.M. & Gabriels D. 2008a. The impact of forest edge structure on longitudinal patterns of deposition, wind speed, and turbulence. *Atmos. Environ.* 42: 8651–8660.

Wuyts K., De Schrijver A., Staelens J., Gielis L., Vanderbruwane J. & Verheyen K. 2008b. Comparison of forest edge effects on throughfall deposition in different forest types. *Environ. Pollut.* 156: 854–861.

Wuyts K., De Schrijver A., Staelens J., Gielis L., Geudens G. & Verheyen K. 2008c. Patterns of throughfall deposition along a transect in forest edges of silver birch and Corsican pine. *Can. J. For. Res.* 38: 449–461.

Wu Y.L., Davidson C.I., Dolske D.A. & Sherwood S.I. 1992. Dry deposition of atmospheric contaminants to surrogate surfaces and vegetation. *Aerosol Sci. Technol.* 16: 65–81.

Appendix. Summary of characteristic parameters for the ten experimental runs.

Run ID	Row or plate no.	u (m s^{-1})	RH (%)	Temp (°C)	Leaf area (m^2)	LAI	Coarse to total		Cl^- aerosol conc. (μequiv m^{-3})	Na^+ aerosol conc. (μequiv m^{-3})	Washed-off Cl^- (μequiv)	Washed-off Na^+ (μequiv)	Deposition rates					
													per ground surface area (μequiv m^{-2} s^{-1})		per unit leaf area (μequiv m^{-2} s^{-1})		per plate surface area (μequiv m^{-2} s^{-1})	
							Cl^-	Na^+					Cl^-	Na^+	Cl^-	Na^+	Cl^-	Na^+
HV1016	All	2	62	23	0.17	1.0	0.24	0.24	111	110	106	72	0.20	0.14	0.042	0.029		
	1				0.03	0.9					28	24	0.05	0.05	0.061	0.051	0.032	0.016
	2				0.03	0.9					14	10	0.03	0.02	0.032	0.024	0.032	0.014
	3				0.04	1.0					18	12	0.03	0.02	0.033	0.023	0.026	0.014
	4				0.03	0.8					11	8.3	0.02	0.02	0.028	0.021		
	5				0.05	1.3					34	17	0.07	0.03	0.052	0.025		
HV1017	All	2	61	23	0.21	1.1	0.25	0.25	137	135	126	86	0.24	0.17	0.043	0.029		
	1				0.03	0.9					28	23	0.05	0.04	0.06	0.049	0.025	0.017
	2				0.05	1.3					26	22	0.05	0.04	0.039	0.033	0.025	0.017
	3				0.05	1.4					30	17	0.06	0.03	0.042	0.024	0.024	0.017
	4				0.04	1.2					29	15	0.06	0.03	0.046	0.024		
	5				0.03	0.9					13	9.1	0.03	0.02	0.028	0.019		
HO0929	All	2	60	23	0.19	1.1	0.29	0.29	80.9	80.2	91	77	0.18	0.15	0.033	0.028		
	1				0.03	0.9					25	21	0.05	0.04	0.05	0.043	0.025	0.014
	2				0.03	0.9					17	14	0.03	0.03	0.036	0.030	0.024	0.013
	3				0.05	1.4					20	16	0.04	0.03	0.028	0.023	0.022	0.012
	4				0.04	1.2					17	15	0.03	0.03	0.029	0.024		
	5				0.03	1.0					13	10	0.02	0.02	0.026	0.021		
HO1001	All	2	60	23	0.18	1.0	0.29	0.29	141	141	117	102	0.22	0.2	0.045	0.039		
	1				0.05	1.3					42	38	0.08	0.07	0.062	0.056	0.030	0.017
	2				0.03	0.9					23	20	0.04	0.04	0.052	0.045	0.031	0.019
	3				0.03	0.8					18	16	0.04	0.03	0.042	0.037	0.029	0.017
	4				0.02	0.5					11	9.5	0.02	0.02	0.038	0.034		
	5				0.05	1.4					23	18	0.04	0.04	0.031	0.025		
HO1020	All	2	59	23	0.31	1.7	0.24	0.25	116	118	108	108	0.21	0.21	0.024	0.024		
	1				0.06	1.7					36	29	0.07	0.06	0.042	0.034	0.018	0.016
	2				0.07	2.0					11	20	0.02	0.04	0.011	0.020	0.018	0.016
	3				0.05	1.4					22	22	0.04	0.04	0.031	0.031	0.016	0.016
	4				0.06	1.5					17	18	0.03	0.04	0.021	0.023		
	5				0.07	2.0					22	19	0.04	0.04	0.021	0.018		

LV1008	All	2	56	23	0.18	1.0	0.32	0.32	40.8	38.4	70	49	0.13	0.09	0.027	0.019		
	1				0.04	1.2					17	14	0.03	0.03	0.027	0.023	0.014	0.008
	2				0.04	1.0					17	11	0.03	0.02	0.031	0.019	0.013	0.008
	3				0.03	0.8					4.6	5.3	0.01	0.01	0.011	0.012	0.013	0.007
	4				0.04	1.1					15	10	0.03	0.02	0.027	0.019		
	5				0.03	0.9					17	8.8	0.03	0.02	0.035	0.018		
LV1010	All	2	59	23	0.23	1.2	0.33	0.32	39.4	39.5	92	61	0.18	0.12	0.028	0.019		
	1				0.04	1.0					18	12	0.03	0.02	0.035	0.023	0.016	0.008
	2				0.05	1.3					18	13	0.03	0.03	0.026	0.019	0.022	0.012
	3				0.05	1.4					21	12	0.04	0.02	0.03	0.017	0.015	0.007
	4				0.04	1.2					15	11	0.03	0.02	0.026	0.019		
	5				0.05	1.4					20	12	0.04	0.02	0.027	0.017		
LO1006	All	2	56	23	0.24	1.3	0.35	0.35	34.6	34.5	71	62	0.14	0.12	0.021	0.018		
	1				0.06	1.6					18	16	0.03	0.03	0.021	0.019	0.014	0.010
	2				0.04	1.2					7.9	6.3	0.02	0.01	0.013	0.01	0.014	0.013
	3				0.05	1.3					13	11	0.03	0.02	0.02	0.017	0.013	0.008
	4				0.04	1.2					11	9.4	0.02	0.02	0.018	0.016		
	5				0.05	1.5					22	19	0.04	0.04	0.029	0.025		
LO1014	All	2	60	23	0.24	1.3	0.32	0.32	44.2	41.8	58	58	0.11	0.11	0.017	0.017		
	1				0.04	1.2					17	16	0.03	0.03	0.028	0.026	0.012	0.009
	2				0.05	1.4					12	12	0.02	0.02	0.018	0.016	0.011	0.009
	3				0.05	1.5					11	13	0.02	0.03	0.014	0.017	0.011	0.009
	4				0.05	1.3					9.8	9.7	0.02	0.02	0.015	0.015		
	5				0.05	1.4					7.8	7.9	0.01	0.02	0.011	0.011		
HO0925	All	2	60	23	0.14	0.8	0.32	0.32	89.2	88.2	77	52	0.15	0.1	0.039	0.026		
	1				0.04	1.1					29	22	0.06	0.04	0.051	0.039	0.020	0.011
	2				0.02	0.7					12	7.0	0.02	0.01	0.034	0.02		
	3				0.03	0.7					12	7.7	0.02	0.01	0.032	0.02		
	4				0.03	0.7					12	8.3	0.02	0.02	0.033	0.022		
	5				0.02	0.6					12	7.0	0.02	0.01	0.04	0.024		